

The Application of Soil-Gas Technique to Geothermal Exploration: Study of Hidden Potential Geothermal Systems

Nunzia Voltattorni, Alessandra Sciarra and Fedora Quattrocchi

Istituto Nazionale di Geofisica e Vulcanologia – Via di Vigna Murata, 605, 00143 Rome (Italy)

nunzia.voltattorni@ingv.it

Keywords: soil-gas technique, flux measurements.

ABSTRACT

Geochemical studies were conducted using soil-gas and flux surveyings for locating both permeable zones in buried reservoirs and the presence of possible gaseous haloes linked to active geothermal systems.

In this work we focused our interest on the distribution of soil-gas concentrations (Rn, Th, He, H₂, O₂, N₂, CO₂, CH₄ and H₂S) in the soil air of the Tetitlan area (Nayarit, Mexico) considered a potential thermal field and characterized by scarcity of surface manifestations.

A total of 154 soil-gas samples and 346 CO₂ and CH₄ flux measurements were collected in an area of about 80 square kilometres. The performed soil-gas and flux geochemical surveys highlighted a general rising patterns linked to local fault system, with the important implication that the highest CO₂ and CH₄ fluxes, as well as Rn concentrations, could be used in undeveloped geothermal systems to identify main upflow regions and areas of increased and deep permeability.

1. INTRODUCTION

The soil-gas method used to infer the nature of subsurface geology/geochemistry is based on the concept that gases which are released from active geothermal systems, can freely rise through overlying cover to be detected in the near-surface. The high mobility of some gases makes them the best pathfinders for concealed natural resources. Indeed, the gases produced and/or accumulated in geothermal reservoirs can escape towards the surface by diffusion, through transportation by rising hot fluids and by migration along fractures and faults. Faults and fractures can favour gas leaks because they usually increase rock and soil permeability, and thus the presence of linear soil-gas anomalies longer than several meters are often taken as strong evidence of tectonic features (Fridman, 1990). It is important to note that faults are typically wide fracture zones that can also be crosscut by other structures, thus resulting in diffuse or “halo” anomalies, respectively (Matthews, 1985; Sokolov, 1971). Recent research has demonstrated that the gas-bearing properties of faults are not necessarily continuous along a tectonic structure (Etiope et al., 2005; Ciotoli et al., 2005; Baubron et al., 2002; Lombardi et al., 1996; Ciotoli et al., 1998; Salvi et al., 2000; Pizzino et al., 2004; Voltattorni et al., 2006). In these cases isolated points with high concentration values (“spotty anomalies”), are frequently observed. When multiple “spot” anomalies occur along a linear trend, one can infer that they lie along a structural feature which has a spatially discontinuous in terms of its gas-bearing properties (Ciotoli et al., 1998; Lombardi et al., 1996). Extensive experience in soil-gas prospecting by the authors indicates that soil gas anomalies generally occur as linear,

fault linked, anomalies, as well as in irregularly shaped diffuse or halo anomalies and irregularly spaced plumes or spot anomalies (Voltattorni et al., 2005; Beaubien et al., 2002; Lombardi and Voltattorni, 2003; Lombardi et al., 1996). These features reflect gas migration dominated by brittle deformation both at macroscale and/or microscale. Therefore spatial patterns of soil-gases in faulted areas appear to be suitable tools for identifying tectonic structures also in areas characterized by thick clay cover whose plastic behaviour could mask the identification of faults by mean of other geological (field mapping) and geophysical methods.

This paper deals with the results of both soil and flux gas prospecting in the Tetitlan area (Nayarit, Mexico), considered a potential thermal field and characterized by scarcity of surface manifestations. The geochemical prospecting was performed in an area of about 80 km² achieving soil-gas samples, radon and thoron measurements, CO₂ and CH₄ flux measurements

2. GEOLOGICAL SETTING

The Tetitlan-Valle Verde thermal area belongs to the San Pedro-Ceboruco graben (SPC), a Neogene structure developed in the western Trans-Mexican Volcanic Belt (TMVB) in the proximity of the southern Gulf of California. The SPC is also a northermost tectonic basin of the so-called Tepic-Zacoalco rift where complex extensional tectonism occurred associated with both Na-alkaline and calc-alkaline volcanism since the late Miocene (Verma and Nelson, 1989a, 1989b; Ferrari et al., 1994, 1997; Righter et al., 1995; Rosas-Elguera et al., 1996; Ferrari and Rosas-Elguera, 2000; Ferrari et al., 2000; Righter, 2000; Petrone et al., 2003).

The SPC is a complex, WNW-ESE striking extensional basin located along the boundary between the Jalisco Block (JB) and the Sierra Madre Occidental to the north. Magmatism was intimately associated with formation of the SPC, with emplacement of volcanic and sub-volcanic bodies at least since Pliocene.

Exploratory wells were drilled for geothermal purposes by the Comisión Federal de Electricidad (CFE) in the SPC. Three deep wells (reached depths of 2700, 1600 and 1900m) indicate the presence of three segments forming the SPC depression (Ferrari et al., 2003): 1) the Compostela graben to the west: it is bounded by two WNW-ESE striking normal fault systems cutting an early Pliocene rhyolitic complex in the north, and Cretaceous to Pliocene ash flows and plutons of the JB in the south; 2) the San Pedro central depression formed by N-S striking faults. The inside developed volcanic structures are younger than the N-S fault system constraining the age of the extension to the middle Pleistocene; and 3) the Ceboruco asymmetric graben to the east: it is bounded to the north by WNW-ESE

striking faults which cut a rhyolitic and ignimbritic succession dated at 4.7 to 4.2 Ma (Righter et al., 1995).

3. METHODS

3.1 Soil-gas sampling and analysis

Soil-gas surveying consists of the collection and analysis of gas samples from the unsaturated, possibly dry, zones. In the present study samples were collected using a stainless steel probe driven into the ground to a depth of 0.5 m; this depth is considered below the major influence of meteorological variables (Hinkle, 1994; Segovia et al., 1987).

Furthermore, the collection of a large number of samples statistically minimizes sampling/analytical error and bias caused by individual samples (Beaubien et al., 2003; Annunziatellis et al., 2003; Lombardi et al., 1996; Hinkle, 1994; Reimer, 1990). Radon and thoron are analyzed immediately in the field, due to their half-life (respectively of 3.8 days for radon and 55 sec for thoron), using a RAD7 Durridge® alpha spectrometry instrument.

Radon (^{222}Rn) and thoron (^{220}Rn) values were measured every 15 minutes (third cycle reliable for the final reading of the two components) pumping from the steel probe. The ionization chamber of the detector is protected by the $> 10\%$ humidity by a “drierite” trap and a “gasoline” type pre-filter. Radon and thoron particles generate positive charged ^{218}Po and ^{216}Po ions after entering the chamber and they are collected on the detector by electrical high-Voltage field sources. Radon calculation is based on the sum of ^{218}Po and ^{214}Po peaks, and thoron calculation is based on ^{216}Po only because of the slow response of $^{212}\text{Bi}/^{212}\text{Po}$.

A 50 ml gas sample was placed in a previously evacuated, 25 ml volume, stainless-steel canister for transport and storage. Once in the laboratory, each gas sample was also analyzed for major (N_2 , O_2 , CO_2) and minor (C_{1-4} hydrocarbon, He , H_2 , H_2S) gas species using a *Perkin-Elmer AutoSystem XL* packed-column gas chromatograph.

A soil-gas survey was performed over the Tetitlan area (about 80 km 2) according to a regional sampling with a density of 4–6 samples km 2 (100 samples, Figure 1, black dots). Furthermore, some high-resolution surveys (54

samples) were performed within detailed zones (Santa Isabel, Valle Verde and Tetitlan villages) across the area to enhance the chances of properly recording the fault gas signal and to study fault influence on shallow soil gas distribution.

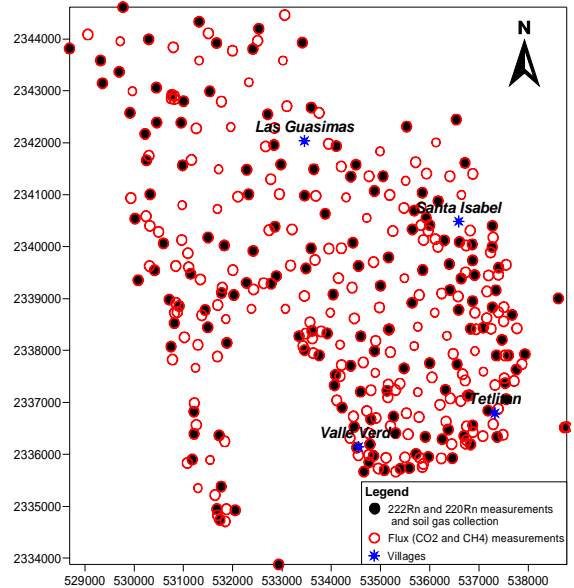


Figure 1: Sampling distribution: soil gas sampling and radon measurements in black dots, flux measurements in red dots.

3.2 Flux measurements

A total of 346 measurements of soil-gas exhalation (CO_2 and CH_4 , Figure 1, red dots) were performed using a speed-portable “closed dynamic” accumulation chamber “time 0” (West System™ instrument). The instrument is equipped of two sensors with different detection limit: 0.01 gr/m 2 day for methane and 0.2 gr/m 2 day for carbon dioxide. Accumulation chamber measurement techniques and flux-calculation methods have been widely described by many authors: Werner et al. (2000), Bergfeld et al. (2001) Chiodini et al. (1995, 1998, 2000), Chiodini and Frondini (2001), Cardellini et al. (2003).

Table 1: The main statistics of soil gas data show that CO_2 , He , H_2 , N_2 , and O_2 have low dispersed distributions as highlighted by the low value of the standard deviation. Otherwise, the wide ranges, as well as the high values of the skewness, for CH_4 and Rn concentrations indicate the presence of outliers. The mean and the median values for CH_4 and Rn highlight that the frequency distribution of these gases are positively skewed, indicating an exponential or lognormal distribution of these variables. In the case of skewed distributions, the median of CH_4 and of Rn , are better than the mean and the standard deviation to provide data dispersion and to highlight values that may be considered as anomalous.

	Samples	Mean	Median	Min Value	Max Value	Lower Quartile	Upper Quartile	Variance	Standard Deviation	Skewness
Radon (Bq/m 3)	154	2702,38	2180,00	0,00	19200,00	1080,00	3490,00	5979312,66	2445,26	3,18
Thoron (Bq/m 3)	154	6830,84	5120,00	289,00	24100,00	2960,00	9770,00	27268498,20	5221,92	1,11
He (ppm)	154	5,62	5,55	4,19	8,20	5,47	5,64	0,21	0,46	3,25
H ₂ (ppm)	154	1,66	1,29	0,54	7,42	1,11	1,70	1,03	1,02	2,94
O ₂ (%)	154	19,88	19,90	19,22	20,56	19,75	20,01	0,04	0,21	-0,39
N ₂ (%)	154	77,38	77,30	76,77	78,68	77,14	77,57	0,13	0,36	1,03
CH ₄ (ppm)	154	30,32	2,54	0,17	653,39	0,85	17,63	8340,08	91,32	4,96
CO ₂ (%)	154	0,19	0,17	0,02	0,87	0,10	0,24	0,02	0,13	2,31

3.3 Data interpretation

Geostatistical techniques were applied for the study of spatially correlated data. Exploratory analysis was first performed to evaluate the basic characteristics of the data (i.e., summary statistics and statistical distribution of each variable).

Univariate and bivariate statistical and graphical methods were used to study each variable independently, the relationship between variable pairs, as well as to highlight the presence of multiple populations.

Exploratory spatial data analysis consisted of preliminary spatial data representation by using classed post maps to show value distribution and to visualize the intersample distance, which is useful to determine the grouping intervals for experimental semivariogram calculation and to choose search radii in estimation routines (kriging). Variogram analysis is performed to check spatial continuity of the data values and the presence of anisotropies. Once spatial continuity is characterized, it is modelled with variogram functions that form the basis for kriging.

4. RESULTS

4.1 Soil-gas concentrations

The exploratory data analysis shows that CO₂, He, H₂, N₂ and O₂ have low dispersed distributions, as highlighted by the low value of the variance (Table 1). Otherwise, the wide ranges, as well as the high skewness values, for CH₄ and Rn indicate the presence of outliers. The mean and median values for CH₄ (30.32 ppm and 2.54 ppm), and Rn (2702.38 Bq/m³ and 2180.00 Bq/m³) highlight that the frequency distribution of these gases are positively skewed (4.96 and 3.18, respectively), indicating an exponential or lognormal distribution.

These preliminary considerations indicate that active gas-bearing faults present in the area favour gas leakage. In particular, the high median values of Rn and CH₄ would confirm the presence of high gas microseeps. The low median values of He, H₂, CO₂ concentrations could be due to dilution by major atmospheric components, i.e., nitrogen and oxygen. Furthermore, dilution by surface gases of biological origin may also alter CO₂ and CH₄ signatures. In this case the shallow distribution of fault-related anomalies of these minor and trace species can be shown by spot values that could show a linear pattern. These soil-gas anomalies, however, may display a complex character, both in space and time.

For example, anomalies may differ according to the structure of the faults, such as fault gouges versus intensely sheared zones, resulting in a different shallow pattern due to the low gas permeability of fault gouge materials compared to high permeability of fractured rocks in the adjacent shear zones (King et al., 1996; Sugisaki et al., 1980). On this basis gas anomalies in correspondence of active faults can be either “direct leak anomalies” indicating a deep gas origin, or “secondary anomalies” linked to the shallower chemical-physical nature of the fault-constituting rocks.

Because soil-gases have a different abundance with respect to the atmospheric air, (0.01 kBq m³ for ²²²Rn, 0.036 for CO₂, 1.4 ppm for CH₄, 5.20 ppm for He, 78.08% for N₂, 19.4% for O₂, 0.5 ppm for H₂), the detection of an anomaly threshold constitutes a fundamental step in the exploratory statistical analysis for further discussion about the possible

sources of the studied gases. Various statistical methods can be applied to assess the anomalies relative to background (Ciotoli et al., 2005; Beaubien et al., 2003; Sinclair, 1991). In general, our experience highlights a strong correspondence between the upper quartile and the anomaly threshold. It should be remembered, however, that soil-gas anomalies cannot be fixed absolutely, but rather must be defined locally due to their complex origins.

According to Sinclair (1991) the normal probability plot (NPP) provides a good method to distinguish different, often overlapping, populations (i.e., background, anomalous values, and outliers) and a more objective approach to statistical anomaly threshold estimation. As an example,

Figure 2 highlights how the anomaly threshold is calculated on the basis of achieved He results. Figure 3 shows the concentration maps of the analysed soil-gas species. Anomalous carbon dioxide values agree well with the radon activity suggesting a fit with supposed local fault systems (Ferrari et al., 2003). This correlation supports the presence of buried gas-bearing channels in the area where the migration of CO₂ acts as carrier for trace species, suggesting a potential deep origin of these gases. This hypothesis is strengthened where methane and helium anomalies are also measured (particularly in the eastern sector, between Santa Isabel and Tetitlan villages and in the north-western sector, in proximity of Cerro San Pedro). However, to reinforce the hypothesis about the origin of CO₂, carbon isotopic analyses are required. The interpretation of CH₄ data is generally complex because this gas can be biologically produced in an-oxic sediments which are commonly rich in organic matter but can be biologically consumed in oxic soils. Figure 3 shows that anomalous values are located mostly in the southern side of the area in correspondence of Valle Verde village. The origin of methane can be interpreted based on isotopic signatures ($\delta^{13}\text{C}$ and associations with other gases, e.g., heavier hydrocarbons). Anomalous values of H₂ often overlap methane ones suggesting a direct chemical correlation between the two soil-gas species. The presence of thoron anomalous values spreading almost all over the sampled area suggests an interesting diffusion in the lower layers of the atmosphere.

In order to study the different contribution of direction-specific versus random phenomena a geostatistical analysis was performed constructing experimental variograms in different direction for a better interpretation of anisotropies. In fact, directional variograms can differ in total sill value, highlighting a false “zonal anisotropy.” For this reason it is recommended to remove the proportional effect by calculating “relative variograms,” where each pair difference is divided by the average of the individual pair of samples.

In linear geostatistics, as in conventional statistics, a normal distribution for the variable under study is desirable. Even though normality may not be strictly required, high skewness and outliers can impair the variogram structure and the kriging results. For this reason, the variographic study was performed only for Rn and CH₄, because they constitute a typical carrier/trace gas association and because they show a less skewed data distribution than the other gases.

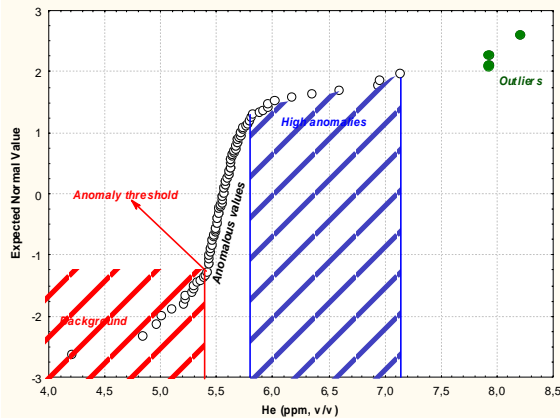


Figure 2: Normal Probability Plot is used to evaluate the normality of the distribution of a variable, that is, whether and to what extent the distribution of the variable follows the normal distribution (in this last case, all values should fall onto a straight line). Data refer to He gas results achieved during the present study.

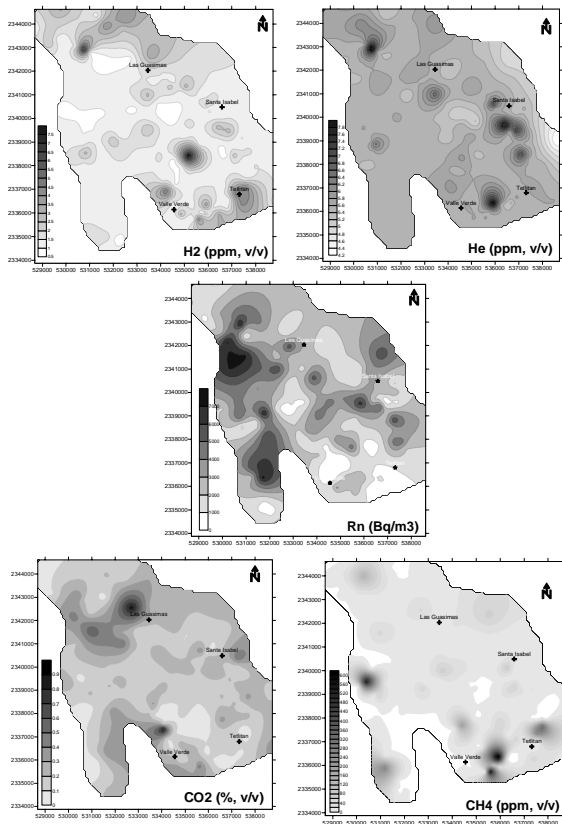


Figure 3: Soil gas concentration maps show a different distribution for each gas specie excepting in the north-western sector of the area where radon and carbon dioxide anomalous values are more concentrated. He, H₂ and CH₄ have a more spotty distribution in the south- eastern sector.

Figure 4 shows the contoured radon and methane values in sampled area using the parameters of the selected variogram models. The experimental variograms of CH₄ and Rn for the northern sector confirm the presence of anisotropy as they reach the same sill value at different

ranges while, for the eastern sector, they highlight a quite different spatial domain showing a more complex structure.

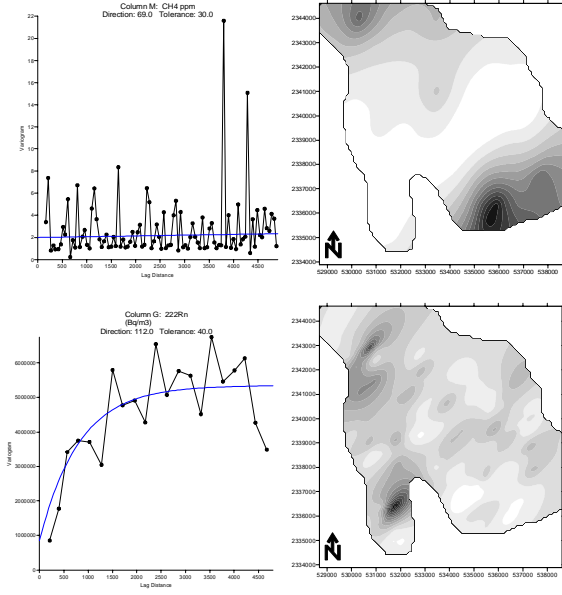


Figure 4: Methane and radon contour maps elaborated on the basis of modelled experimental variograms. The methane map highlights a major anomaly both in the southern and northern sector north oriented. On the contrary, the radon anomalies are evident along the western part of the studied area.

4.1 Soil-gas fluxes

Carbon dioxide and methane fluxes were measured at 346 locations. Measurement spacing varied between 100 and 250 m including locations where soil-gas concentration measurements were made at the same time. Data achieved directly on the field, were treated and calculated considering the variation of barometric pressure and temperature measured during the survey. Fluxes were analyzed using experimental variograms computed and modelled both for methane and carbon dioxide. Emission rates for each realization were calculated by summing the simulated flux across the grid and multiplying by the grid area. The average and standard deviations of the emission rates reported in Table 2 are calculated from the flux realizations.

Table 2: Main Statistics of Soil Gas Fluxes

Flux	N° samples	Mean	Median	Min Value	Max Value	Std. Dev.	CV*
CO ₂ (g/m ² d)	346	2,18	1,34	0,00	45,14	4,39	2,02
CH ₄ (g/m ² d)	346	0,83	0,55	0,00	9,00	1,02	1,24

*CV, coefficient of variation (standard deviation divided by the mean).

Carbon dioxide and methane fluxes ranged from not detectable (<3 g/m² d⁻¹) to 45,14 g/m² d⁻¹ and to 9,00 g/m² d⁻¹ respectively. The means of the entire CO₂ and CH₄ flux data set were 2.19 and 0.83 g/m² d⁻¹, respectively. The data set had a coefficient of variation (CV: the standard deviation divided by the mean) of 2,02 for CO₂ and 1,24 for CH₄, where CV values greater than 1 indicate a non-normal, potentially log-normal, population distribution (Singh and Engelhardt, 1997). The distributions of fluxes within the area were skewed suggesting that CO₂ and CH₄ fluxes are spatially variable across the study area.

The contour maps (Figure 5) elaborated on the basis of the calculated experimental variograms, demonstrate that gas emission at the surface is not spatially heterogeneous within studied area. It is possible to infer that the variability of gas emissions is controlled by geological structures.

A comparison between the radon concentration map and the CH_4 flux distribution map (Figure 6) highlights an overlapping of the anomalous values: the methane flux acts as carrier gas for the radon rising along preferential pathways both in the north-western sector and in the central part of the area as well as the north-eastern.

5. CONCLUSIONS

In the surveyed area of Tetitlan (Nayarit, Mexico), considered a potential thermal field and characterized by scarcity of surface manifestations, both soil-gas survey and flux measurements had the aim to select permeable zones at depth.

The soil-gas surveys, carried out in April 2008, suggest a division of the prospected region in different parts: the largest areas of degassing were observed to the north-western of Las Guasimas village and in a large area surrounding the Santa Isabel village. Furthermore, some spot anomalies were found in proximity of Tetitlan and Valle Verde villages. The rest of the area is characterised by low or absent soil-gas and flux anomalies.

The spatial pattern of the main CO_2 , CH_4 flux anomalies as well as Rn , CO_2 , CH_4 and He soil-gas anomalies suggests a structural control on degassing. In particular, the convergence of different gas species (Rn and CH_4) anomalies indicate zones where better permeability can occur at depth.

Further investigations including a more detailed soil gas and flux surveys (e.g., local transects with a major spatial sampling density) are suggested in order to better understand the nature of spot anomalies. Moreover, it is strictly recommended to collect samples for isotopic analysis (in particular, $\delta^{13}\text{C}$) both for methane and carbon dioxide so as to understand and define the origin of such gas species and, consequently, to give a more detailed interpretation of achieved data.

ACKNOWLEDGMENTS

The authors would like to thank the Comisiòn Federal de Electricidad (CFE) for all bibliographic material. The efforts of Dr. Francisco Gonzales Sanchez and Don Pedro who facilitated data collection, were greatly appreciated as well as the logistic support provided by Dr Antoni Camprubì from UNAM, Mexico City.

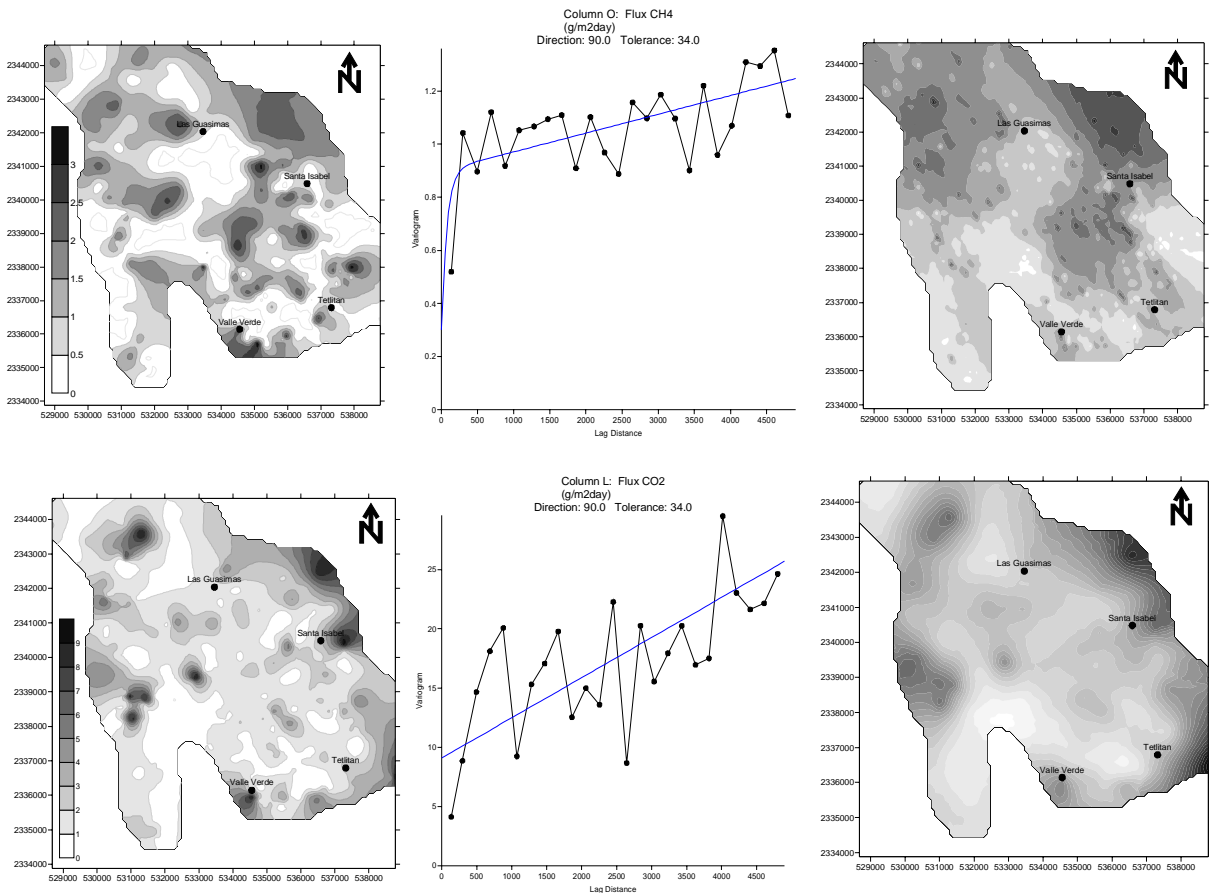


Figure 5: CO_2 and CH_4 flux concentration maps (on the left) and contour maps (on the right) elaborated on the basis of calculated experimental variograms. According to the latter maps, the methane flux is more evident in the north-western sector and in the central part of the area as well as the north-eastern. The carbon dioxide flux follow almost the same directions but has a more diffusive behaviour.

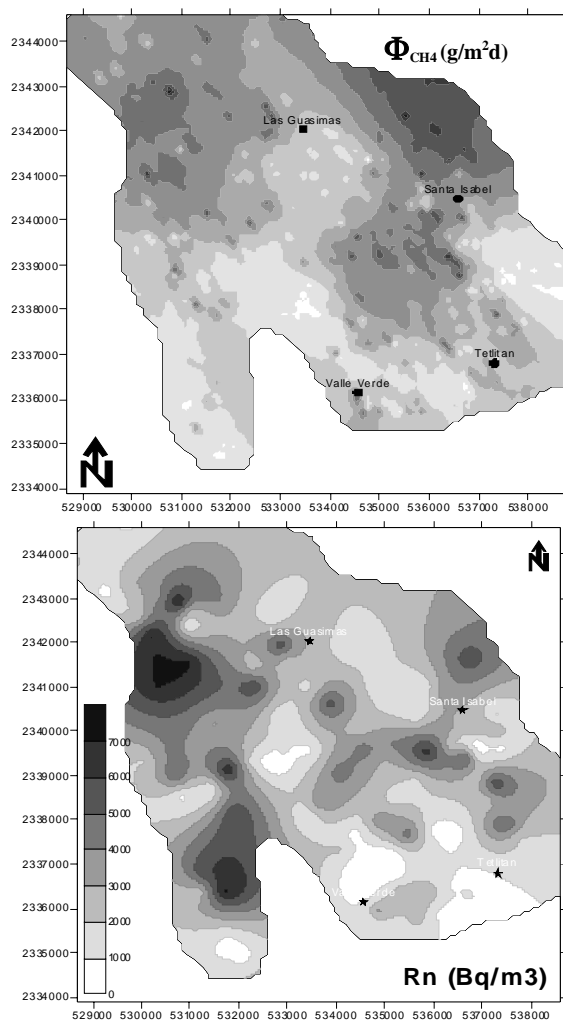


Figure 6: A comparison between the CH_4 flux distribution map (at the right) and the radon concentration map (at the left). There is a good overlapping of the gas anomalous values to NW of Las Guasimas and in the central part of the area as well as in the north-eastern (between Santa Isabel and Tetlitan villages) sector of the studied area.

REFERENCES

Annunziatellis, A., G. Ciotoli, S. Lombardi, and Nolasco F.: Short and long term gas hazard: The release of toxic gases in the Alban Hills volcanic area (central Italy), *J. Geochem. Explor.*, **77**, (2003), 93-108.

Baubron, J. C., Rigo, A., and Toutain, J. P.: Soil gas profiles as a tool to characterize active tectonic areas: The Jaut Pass example (Pyrenees, France), *Earth Planet. Sci. Lett.*, **196**, (2002), 69-81.

Beaubien, S.E., Lombardi, S., and Voltattorni, N.: Radon studies for investigation of nuclear waste deposits and natural emissions. In: "Lake Issyk-kul: Its Natural Environment". Edited by J. Klerks & B. Imanackunov . Nato Science Series, IV. Earth and Environmental Sciences, **13**, (2002), 245-260.

Beaubien, S. E., Ciotoli, G., and Lombardi, S.: Carbon dioxide and radon gas hazard at the Alban Hill Area (central Italy), *J. Volcanol. Geotherm. Res.*, **123**, (2003), 63-80.

Bergfeld, D., Goff, F., and Allard, P.: Preface - high CO_2 flux measurements in volcanic and geothermal areas, methodologies and results. *Chem. Geol.*, **177**, (2001), 1-2.

Cardellini, C., Chiodini, G., and Frondini, F.: Application of stochastic simulation to CO_2 flux from soil: mapping and quantification of gas release. *J.G.R.*, **108** (B9), (2003), 2425-2438.

Chiodini, G., Frondini, F., and Ponziani F.: Deep structures and carbon dioxide degassing in Central Italy, *Geothermics*, **24**, (1995), 81-94.

Chiodini, G., Cioni, R., Guidi, M., Raco, B., and Marini, L.: Soil CO_2 flux measurements in volcanic and geothermal areas, *Applied Geochemistry*, **13** (5), (1998), 543-552.

Chiodini, G., Frondini, F., Cardellini, C., Parello, C., and Peruzzi, L.: Rate of diffuse carbon dioxide. Earth degassing estimated from carbon balance of regional aquifers: the case of central Apennines, Italy, *J.G.R.*, **105** (B4), (2000), 8423-8434.

Chiodini, G., and Frondini, F.: Carbon dioxide degassing from the Albani Hills volcanic region, Central Italy. *Chemical Geology*, **177**, (2001), 67-83.

Ciotoli, G., Guerra, M., Lombardi, S., and Vittori, E.: Soil gas survey for tracing seismogenic faults: A case study in the Fucino Basin, central Italy, *J. Geophys. Res.*, **103**, (1998), 23,781- 23,794.

Ciotoli, G., Lombardi, S., Morandi, S., and Zarlenza, F.: A multidisciplinary statistical approach to study the relationships between helium leakage and neo-tectonic activity in a gas province: The Vasto Basin, Abruzzo-Molise (central Italy), *AAPG Bull.*, **88** (3), (2005), 355-372.

Etiope, G., Guerra, M., and Raschi, A.: Carbon dioxide and radon geohazards over a gas-bearing fault in the Siena graben (central Italy), *TAO*, **16** (4), (2005), 885- 896.

Ferrari, L., Pasquare, G., Venegas, S., Castello, D., and Romero, F.: Regional tectonics of western Mexico and its implications for the northern boundary of the Jalisco Block. *Geofisica International*, **33**, (1994), 139-151.

Ferrari, L., Nelson, S.A., Rosas-Elguera, J., Aguirre-Diaz, G., and Venegas-Salgado, S.: Tectonics and volcanism of the Western Mexican Volcanic Belt. In: Aguirre-Diaz, G.J., Aranda-Gomez, J.J., Carrasco-Nunez, G., Ferrari, L. (Eds.), *Magma and Tectonics in Central and North-Western Mexico —A Selection of the 1997 IAVCEI General Assembly Excursions*, Mexico DF, Excursions, **12**, (1997), 85-129.

Ferrari, L., and Rosas-Elguera, J.: Late Miocene to Quaternary extension at the northern boundary of the Jalisco block, western Mexico: the Tepic- Zacoalco rift revised. *Geol. Soc. Am., Spec.Pap.*, **334**, (2000), 41-64 (Chap. 03).

Ferrari, L., Pasquare, G., Vanegas-Salgado, S., and Romero-Rios, F.: Geology of the western Mexican Volcanic Belt and adjacent Sierra Madre Occidental and Jalisco Block. *Geol. Soc. Am., Spec. Pap.*, **334**, (2000), 65-84 (Chap. 04).

Ferrari, L., Petrone, C.M., Francalanci, L., Tagami, T., Eguchi, M., Ponticelli, S., Manetti, P., and Venegas-Salgado, S.: Geology of the San Pedro-Ceboruco graben, western trans-mexican volcanic belt. *Revista Mexicana de Ciencias Geologicas*, **20** (3), (2003), 165-181.

Fridman, A. I.: Application of naturally occurring gases as geochemical pathfinders in prospecting for endogenous deposits, *J. Geochem. Explor.*, **38**, (1990), 1-11.

Hinkle, M.: Environmental conditions affecting concentrations of He , CO_2 , O_2 and N_2 in soil gases, *Appl. Geochem.*, **9**, (1994), 53- 63.

King, C.Y., King, B.S., Evans, W.C., and Zang, W.: Spatial radon anomalies on active faults in California, *Appl. Geochem.*, **11**, (1996), 497–510.

Lombardi, S.: The refinement of soil gas analysis as a geological investigative technique, in 4th CEC R&D Programme on Management and Storage of Radioactive Waste (1990 – 1994), final report, Nucl. Sci. Technol. Ser. EUR 16929, (1996), 193 pp., Eur. Comm., Brussels.

Lombardi, S., and Voltattorni, N.: Study of a Natural Analogue of the Thermo-hydro-chemical and Thermo-hydro-mechanical Response of Clay Barriers: the Orciatico area (Tuscany, Central Italy) EGS-AGU-EUG Joint Assembly, Nice, France, 6-11 April. *Geoph. Res. Abs.*, **5**, (2003), NH 10.

Matthews, M. D.: Effects of hydrocarbon leakage on Earth surface materials, in Unconventional Methods in Exploration for Petroleum and Natural Gas, IV, edited by M. J. Davidson, (1985), 27– 44, South. Methodist Univ. Press, Dallas, Tex.

Petrone, C.M., Francalanci, L., Carlson, R.W., Ferrari, L., and Ponticelli, S.: Unusual coexistence of subduction-related and intraplate-type magmatism: Sr, Nd and Pb isotope and trace elements data from the magmatism of the San Pedro-Ceboruco graben (Nayrit, Mexico). *Chemical Geology*, **193**, (2003), 1-24.

Pizzino, L., Burrato, P., Quattrocchi, F., and Valensise, G.: Geochemical signature of large active faults: the example of the 5 February 1783, Calabrian Earthquake. *Journal of Seismology*, **8**, (2004), 363-380.

Reimer, G.M.: Reconnaissance techniques for determining soil-gas radon concentrations: An example from Prince Georges County, Maryland, *Geophys. Res. Lett.*, **17**, (1990), 809–812.

Righter, K., Carmichael, I.S.E. and Becker, T.: Pliocene-Quaternary faulting and volcanism at the intersection of the Gulf of California and the Mexican Volcanic Belt. *Geological Society of America Bulletin*, **107**, (1995), 612-6237.

Righter, K.: A comparison of basaltic volcanism in the Cascades and western Mexico: compositional diversity in continental arcs. *Tectonophysics*, **318**, (2000), 99-117.

Rosas-Elguera, J., Ferrari, L., Garduno, V.H., and Urrutia-Fucugauchi, J.: The continental boundaries of the Jalisco Block and their influence on the plio-Quaternary kinematics of western Mexico. *Geology*, **24**, (1996), 921-924.

Salvi, S., Quattrocchi, F., Angelone, M., Brunori, C.A., Billi, A., Buongiorno, F., Doumaz, F., Funiciello, R., Guerra, M., Lombardi, S., Mele, G., Pizzino, L., and Salvini, F.: A multidisciplinary approach to earthquake research: implementation of a Geochemical Geographic Information System for the Gargano site, Southern Italy. *Natural Hazard*, **20** (1), (2000), 255-278.

Segovia, N., Seidel, J. L., and Monnin, M.: Variations of radon in soils induced by external factors, *J. Radioanal. Nucl. Chem. Lett.*, **119**, (1987), 199– 209.

Singh, A.K. and Engelhardt, M.: The lognormal distribution in environmental applications. EPA/600/R-97/066. Environmental Protection Agency, Washington, DC. (1997)

Sinclair, A.J.: A fundamental approach to threshold estimation in exploration geochemistry: Probability plots revisited, *J. Geochem. Explor.*, **41**, (1991), 1– 22.

Sokolov, V.A.: Geochemistry of Natural Gases, Niedra, Moscow, (1971).

Sugisaki, R., Anno, H., Aedachi, M., and Ui, H.: Geochemical features of gases and rocks along active faults, *Geochem. J.*, **36**, (1980), 101–112.

Verma, S.P., and Nelson, S.A.: Isotopic and trace element constraints on the origin and evolution of alkalin and calc-alkaline magmas in the northwestern Mexican Volcanic Belt. *J. Geoph. Res.*, **94**, (1989a), 4531-4544.

Verma, S.P., and Nelson, S.A.: Correction to “Isotopic and trace element constraints on the origin and evolution of alkalin and calc-alkaline magmas in the northwestern Mexican Volcanic Belt”. *J. Geoph. Res.*, **96**, (1989b), 7679-7681.

Voltattorni, N., Caramanna, G., Cinti, D., Galli, G., Pizzino, L., and Quattrocchi, F.: Study of CO₂ natural emissions in different Italian geological scenarios: a refinement of natural hazard and risk assessment. In: “Advances in the Geological Storage of Carbon Dioxide, eds. Lombardi S., Altunina L.K. and Beaubien S.E., NATO Science Series, Springer Publishing, Berlin, 2006, XV, 362 p., Softcover. ISBN: 1-4020-4470-4, (2005).

Werner, C., Brantley, S.L., and Boomer, K.: CO₂ emissions related to the Yellowstone volcanic system. 2. Statistical sampling, total degassing, and transport mechanisms. *J. Geophys. Res.*, **105**, (B5), (2000), 10831–10846.